

TWO-NUCLEON SPECTRAL FUNCTION IN INFINITE NUCLEAR MATTER

Omar Benhar

INFN, Sezione Roma 1, I-00185 Rome, Italy

Adelchi Fabrocini

INFN and Dip.di Fisica, Università di Pisa, I-56100 Pisa, Italy

Abstract

The two-nucleon spectral function in nuclear matter is studied using Correlated Basis Function perturbation theory, including central and tensor correlations produced by a realistic hamiltonian. The factorization property of the two-nucleon momentum distribution into the product of the two single nucleon distributions shows up in an analogous property of the spectral function. The correlated model yields a two-hole contribution quenched with respect to Fermi gas model, while the peaks acquire a quasiparticle width that vanishes as the two momenta approach k_F . In addition, three-hole one-particle and more complicated intermediate states give rise to a background, spread out in energy and absent in the uncorrelated models. The possible connections with one- and two-nucleon emission processes are briefly discussed.

Key words: Nuclear structure. Nuclear matter. Two-nucleon emission.

1 Introduction

The two-nucleon spectral function, yielding the probability to remove two nucleons with momenta \mathbf{k}_1 and \mathbf{k}_2 from nuclear matter leaving the residual system with excitation energy E , is defined as (see, e.g., ref.[1]):

$$P(\mathbf{k}_1, \mathbf{k}_2, E) = \sum_n |\langle \bar{0} | a_{\mathbf{k}_1}^\dagger a_{\mathbf{k}_2}^\dagger | \bar{n}(A-2) \rangle|^2 \delta(E - E_n(A-2) + E_0(A)), \quad (1)$$

where $|\bar{0}\rangle$ is the A -particle nuclear matter ground state with energy $E_0(A)$, $|\bar{n}(A-2)\rangle$ denotes a $(A-2)$ -nucleon intermediate state with energy $E_n(A-2)$ and $a_{\mathbf{k}}^\dagger$ is the usual creation operator.

The two-nucleon spectral function carries relevant information on the short range structure of the nuclear medium and nucleon-nucleon (NN) correlations. Therefore, a considerable effort aimed at extracting experimental information on $P(\mathbf{k}_1, \mathbf{k}_2, E)$ is currently being undertaken. In this context, a very important role is played by electron-nucleus scattering experiments (a number of theoretical and experimental topics in the field of electron-nucleus scattering are reviewed in ref.[2]).

Unambiguous evidence of strong correlation effects has been provided by single nucleon knock out ($e, e'p$) reactions, showing that in a nucleus only about 70 % of the nucleons are in states of low momentum and low removal energy, that can be described by a mean field theory. The remaining 30 % of the nucleons belong to strongly correlated pairs, whose occurrence is mainly to be ascribed to the one-pion-exchange tensor force and to the repulsive core of the NN interaction.

The available ($e, e'p$) data at low missing momentum and low missing energy clearly show the depletion of the occupation probabilities of single particle states predicted by the nuclear shell model (for a recent review see, e.g., ref.[3]), thus providing a somewhat indirect measurement of correlation effects. Complementary information will soon be available from single nucleon knock out experiments specifically designed to investigate the kinematical region corresponding to large missing momentum and large missing energy, where correlation effects are believed to be dominant[4].

Over the past decade, the availability of a new generation of high energy 100 % duty-cycle electron beams has made it possible to carry out double coincidence ($e, e'NN$) experiments, in which two knocked out nucleons are detected. In principle, these experiments may allow for direct measurements of *correlation observables*, such as the momentum space two-nucleon distribution or the two-nucleon spectral function. However, as pointed out in ref.[5], extracting the relevant dynamical information from the measured ($e, e'NN$) cross section may turn out to be a challenging task, requiring both a careful choice of the kinematical setup and a quantitative theoretical understanding of the final state interactions (FSI) of the knocked out nucleons.

Regardless of the difficulties involved in the interpretation of the experimental data, reliable theoretical calculations of the two-nucleon emission cross section carried out within the Plane Wave Impulse Approximation (PWIA), in which all the nuclear structure information is contained in the two-nucleon spectral function, have to be regarded as a minimal starting point, which can provide guidance for the optimization of future experiments.

The basic assumptions underlying the PWIA scheme are that i) the exchanged virtual photon couples to either of the two outgoing nucleons and ii) FSI effects

are negligible. The PWIA cross section of the process in which an electron of initial energy E_i is scattered into the solid angle Ω_e with energy $E_f = E_i - \omega$, while two nucleons of kinetic energies T_p and T'_p are ejected into the solid angles Ω_p and Ω'_p , respectively, takes the simple factorized form

$$\frac{d^9\sigma}{d\omega d\Omega_e d\Omega_p dT_p d\Omega'_p dT'_p} = p(T_p + m)p'(T'_p + m)\sigma_{em}F_{\mathbf{p}\mathbf{p}'}(p_m, E_m), \quad (2)$$

where σ_{em} describes the structure of the electromagnetic vertex, m is the nucleon mass and \mathbf{p} and \mathbf{p}' denote the momenta of the detected nucleons. The missing momentum \mathbf{p}_m and missing energy E_m are defined as

$$\mathbf{p}_m = \mathbf{q} - \mathbf{p} - \mathbf{p}', \quad (3)$$

\mathbf{q} being the momentum transfer, and

$$E_m = \omega - T_p - T'_p - T_R, \quad (4)$$

where T_R is the kinetic energy of the recoiling $(A - 2)$ -particle system. The function $F_{\mathbf{p}\mathbf{p}'}(p_m, E_m)$ appearing in eq.(2) can be written in terms of the two-nucleon spectral functions $P(\mathbf{p} - \mathbf{q}, \mathbf{p}', E_m)$ and $P(\mathbf{p}, \mathbf{p}' - \mathbf{q}, E_m)$.

Pioneering studies of the PWIA two-nucleon emission cross section of the $^{12}\text{C}(e, e'pp)$ reaction are discussed in ref.[6], whereas a G-matrix perturbation theory calculation of the ^{16}O two-proton spectral function is described in ref.[7].

In this paper we discuss a calculation of the nuclear matter $P(\mathbf{k}_1, \mathbf{k}_2, E)$ performed using Correlated Basis Function (CBF) perturbation theory. Our theoretical approach, in which the effects of the nonperturbative components of the NN interaction are incorporated in the basis function using a variational approach, has proved to be particularly suited to describe quantities which are strongly affected by NN correlations, such as the single nucleon spectral function $P(\mathbf{k}, E)$ [8], the nucleon momentum distribution $n(\mathbf{k})$ [9] and the off-diagonal density matrix $\rho(\mathbf{r}_1, \mathbf{r}'_1)$ [10].

Following ref.[8], we evaluate the dominant contributions to $P(\mathbf{k}_1, \mathbf{k}_2, E)$ at the zero-th order of CBF, as well as the perturbative corrections that have been shown to be relevant in the calculation of $P(\mathbf{k}, E)$.

CBF theory of infinite nuclear matter is built on the set of *correlated* states:

$$|N\rangle = \mathcal{S} \left[\prod_{i<j} F(i, j) \right] |N\rangle_{FG}, \quad (5)$$

obtained by applying a symmetrized product of two-body correlation operators, $F(i, j)$, to the Fermi gas states $|N\rangle_{FG}$. The structure of $F(i, j)$ is similar to that of the NN interaction:

$$F(i, j) = \sum_n f^{(n)}(r_{ij}) O^{(n)}(i, j) . \quad (6)$$

The operators $O^{(n)}(i, j)$ include four central components $(1, (\sigma_i \cdot \sigma_j), (\tau_i \cdot \tau_j), (\sigma_i \cdot \sigma_j)(\tau_i \cdot \tau_j))$ for $n = 1, 4$ and the isoscalar and isovector tensor ones S_{ij} and $S_{ij}(\tau_i \cdot \tau_j)$ for $n = 5, 6$. Additional spin-orbit components are sometimes introduced, but we will neglect them in this work. With transparent and widely employed notation, the components are also denoted as c ($n = 1$), σ , τ and t (tensor).

Realistic correlated basis states are expected to be close to the eigenstates of the hamiltonian. An efficient recipe to choose the correlation functions consists in their variational determination by minimizing the expectation value of the hamiltonian in the correlated ground state:

$$E_0^v = \langle 0|H|0\rangle . \quad (7)$$

The scalar (or Jastrow) component $f^{(n=1)}(r)$ heals to unity for $r \rightarrow \infty$, whereas $f^{(n \neq 1)}(r) \rightarrow 0$. The tensor components have the longest range, since they are related to the one-pion exchange potential and $F^\dagger(i, j)H_{ij}F(i, j)$ (H_{ij} is the hamiltonian associated with a two-nucleon pair) is a *well-behaved* operator healing to H_{ij} at large interparticle distances, like the G-matrix. The results presented in this work have been obtained using the Urbana v_{14} potential supplemented by the TNI three-nucleon interaction [11].

At the zero-th (or *variational*) order of CBF, $P_{var}(\mathbf{k}_1, \mathbf{k}_2, E)$ is obtained using the correlated states (5) in eq.(1). The variational estimate is then corrected by inserting perturbative corrections in the correlated basis. This procedure has been already adopted for many nuclear matter properties and it has been particularly successful in describing inclusive electromagnetic responses at both intermediate and high momentum transfers (see, e.g., ref.[2]).

In Section 2 we will discuss the relationships between the two-nucleon spectral function, the two-nucleon momentum distribution, and the two-body density matrix, $\rho(\mathbf{r}_1, \mathbf{r}_2; \mathbf{r}'_1, \mathbf{r}'_2)$. Section 3 will present theory and results for the variational two-nucleon spectral function, as well as the main CBF perturbative corrections, evaluated with realistic interactions. Finally, Section 4 is devoted to conclusions and perspectives.

2 Spectral functions, momentum distributions and density matrices

The nuclear matter two-body density matrix $\rho(\mathbf{r}_1, \mathbf{r}_2; \mathbf{r}'_1, \mathbf{r}'_2)$ is defined as

$$\rho(\mathbf{r}_1, \mathbf{r}_2; \mathbf{r}'_1, \mathbf{r}'_2) = A(A-1) \times \frac{\int d^3r_3 \dots d^3r_A \Psi_0^\dagger(\mathbf{r}_1, \mathbf{r}_2, \dots, \mathbf{r}_A) \Psi_0(\mathbf{r}'_1, \mathbf{r}'_2, \dots, \mathbf{r}_A)}{\int d^3r_1 \dots d^3r_A |\Psi_0(\mathbf{r}_1, \mathbf{r}_2, \dots, \mathbf{r}_A)|^2}, \quad (8)$$

$\Psi_0(\mathbf{r}_1, \mathbf{r}_2, \dots, \mathbf{r}_A)$ being the ground state wave function. For $\mathbf{r}_1 = \mathbf{r}'_1$ and $\mathbf{r}_2 = \mathbf{r}'_2$, the density matrix reduces to the two-nucleon density distribution $\rho(\mathbf{r}_1, \mathbf{r}_2)$, yielding the joint probability of finding two nucleons at positions \mathbf{r}_1 and \mathbf{r}_2 in the nuclear matter ground state.

The two-nucleon momentum distribution, i.e. the probability that two nucleons carry momenta \mathbf{k}_1 and \mathbf{k}_2 , is related to the two-nucleon spectral function $P(\mathbf{k}_1, \mathbf{k}_2, E)$, defined in eq.(1), through

$$n(\mathbf{k}_1, \mathbf{k}_2) = \int dE P(\mathbf{k}_1, \mathbf{k}_2, E) = \langle \bar{0} | a_{\mathbf{k}_1}^\dagger a_{\mathbf{k}_2}^\dagger a_{\mathbf{k}_2} a_{\mathbf{k}_1} | \bar{0} \rangle. \quad (9)$$

From Eqs.(8) and (9) it follows that $n(\mathbf{k}_1, \mathbf{k}_2)$ can be written in terms of the density matrix according to

$$n(\mathbf{k}_1, \mathbf{k}_2) = \frac{1}{\nu^2} \frac{1}{\Omega^2} \int d^3r_1 d^3r_2 d^3r'_1 d^3r'_2 e^{i\mathbf{k}_1 \cdot \mathbf{r}_{11'}} e^{i\mathbf{k}_2 \cdot \mathbf{r}_{22'}} \rho(\mathbf{r}_1, \mathbf{r}_2; \mathbf{r}'_1, \mathbf{r}'_2), \quad (10)$$

where ν denotes the degeneracy of the system (in symmetric nuclear matter $\nu = 4$), Ω is the normalization volume, $\mathbf{r}_{11'} = \mathbf{r}_1 - \mathbf{r}'_1$ and $\mathbf{r}_{22'} = \mathbf{r}_2 - \mathbf{r}'_2$.

It is well known[12] that in a Fermi liquid *with no long range order* the two-nucleon momentum distribution factorizes according to

$$n(\mathbf{k}_1, \mathbf{k}_2) = n(\mathbf{k}_1)n(\mathbf{k}_2) + O\left(\frac{1}{A}\right), \quad (11)$$

where $n(\mathbf{k})$ is the single nucleon momentum distribution, defined as

$$n(\mathbf{k}) = \langle \bar{0} | a_{\mathbf{k}}^\dagger a_{\mathbf{k}} | \bar{0} \rangle. \quad (12)$$

The $n(\mathbf{k})$ resulting from the nuclear matter calculation of ref.[9] is shown in fig. 1. It exhibits a discontinuity at $|\mathbf{k}| = k_F$ (the Fermi momentum k_F is related to the density $\rho = A/\Omega$ through $k_F = (6\pi^2\rho/\nu)^{1/3}$), and a tail, extending to

very large momenta, reflecting the structure of the nuclear wave function at small interparticle distance. Eq.(11) implies that in the $A \rightarrow \infty$ limit $n(\mathbf{k}_1, \mathbf{k}_2)$ contains the same dynamical information carried by $n(\mathbf{k})$.

Some insight on the role of short range correlations can be obtained rewriting $n(\mathbf{k}_1, \mathbf{k}_2)$ in terms of the relative and center of mass momenta of the pair, defined as $\mathbf{q} = (\mathbf{k}_1 - \mathbf{k}_2)/2$ and $\mathbf{Q} = \mathbf{k}_1 + \mathbf{k}_2$, respectively, and studying the quantity

$$n_{rel}(\mathbf{q}) = 4\pi|\mathbf{q}|^2 \int d^3Q n\left(\left|\frac{\mathbf{Q}}{2} + \mathbf{q}\right|\right) n\left(\left|\frac{\mathbf{Q}}{2} - \mathbf{q}\right|\right). \quad (13)$$

Fig. 2 illustrates the behaviour of $n_{rel}(\mathbf{q})$ at saturation density (corresponding to $k_F = 1.33 \text{ fm}^{-1}$), evaluated using the momentum distribution of ref.[9] (solid line), compared to the prediction of the Fermi gas model (dashed line).

The inclusion of NN interactions leads to a quenching of the peak, located at $|\mathbf{q}| \sim 0.7\text{-}0.8 \text{ fm}^{-1}$, and to the appearance of a sizeable tail at $|\mathbf{q}| > k_F$. It is interesting to single out the contributions to $n_{rel}(\mathbf{q})$ corresponding to $\mathbf{k}_1, \mathbf{k}_2 < k_F$, $\mathbf{k}_1 < k_F$ and $\mathbf{k}_2 > k_F$, and $\mathbf{k}_1, \mathbf{k}_2 > k_F$. They are represented in fig. 2 by diamonds, squares and crosses, respectively (note that the results shown by the crosses have been enhanced by a factor 10). The $\mathbf{k}_1, \mathbf{k}_2 < k_F$ component provides about 72 % of the normalization of $n_{rel}(\mathbf{q})$ and becomes vanishingly small at $|\mathbf{q}| > k_F$. On the other hand, the contributions coming from pairs in which at least one of the nucleon momenta is larger than k_F are much smaller in size (the curves marked with squares and crosses yield 26 % and 2 % of the normalization, respectively) but extend up to $|\mathbf{q}| \sim 4 \text{ fm}^{-1}$. Similar results have been recently obtained [13] using the momentum distribution resulting from a G-matrix perturbation theory calculation [14].

3 CBF calculation of the two-nucleon spectral function

The propagation of two hole states in nuclear matter is described by the hole-hole part of the two-body Green's function[1],

$$G_{hh}(\mathbf{k}_1, \mathbf{k}_2, E) = \langle \bar{0} | a_{\mathbf{k}_1}^\dagger a_{\mathbf{k}_2}^\dagger \frac{1}{H - E_0 - E - i\eta} a_{\mathbf{k}_2} a_{\mathbf{k}_1} | \bar{0} \rangle, \quad (14)$$

where H is the nuclear matter hamiltonian. G_{hh} is defined for $\epsilon(= -E) < 2e_F$, e_F being the Fermi energy.

The two-nucleon spectral function, given in eq.(1), is straightforwardly related to the imaginary part of G_{hh} by

$$P(\mathbf{k}_1, \mathbf{k}_2, E) = \frac{1}{\pi} \Im G_{hh}(\mathbf{k}_1, \mathbf{k}_2, E) . \quad (15)$$

CBF perturbation theory employs the set of correlated states given in eq.(5). Note that the basis states are non orthogonal to each other. Orthogonalization can be implemented using the procedure proposed in ref.[15], which preserves the diagonal matrix elements of the hamiltonian between correlated states. This technique has been succesfully applied to the calculation of the one-body spectral function in ref.[8] (hereafter denoted I).

The perturbative expansion is obtained separating the nuclear hamiltonian H into two parts: $H = H_0 + H_I$, and using standard Rayleigh-Schrödinger type expansions. The unperturbed and interaction terms, denoted by H_0 and H_I , respectively, are defined through

$$\langle N|H_0|M\rangle = \delta_{NM}\langle N|H_0|N\rangle = \delta_{NM}E_N^v , \quad (16)$$

$$\langle N|H_I|M\rangle = (1 - \delta_{NM})\langle N|H_I|M\rangle . \quad (17)$$

The expectation value in eq.(14) is calculated by expanding

$$|\bar{0}\rangle = \frac{\sum_n (-)^n [(H_0 - E_0^v)^{-1} (H_I - \Delta E_0)]^n |0\rangle}{|\langle \bar{0}|\bar{0}\rangle|^{1/2}} , \quad (18)$$

where $\Delta E_0 = E_0 - E_0^v$. Perturbative corrections to the intermediate states $|N\rangle$ are taken into account carrying out an analogous expansion in powers of $(H_I - \Delta E_0)$ for the propagator appearing in eq.(14), as discussed in I:

$$\frac{1}{(H - E_0 - E - i\eta)} = \frac{1}{(H - E_0^v - E - i\eta)} \times \sum_n (-)^n \left\{ (H_I - \Delta E_0) \frac{1}{(H - E_0^v - E - i\eta)} \right\}^n . \quad (19)$$

We will now describe the structure of the $n = 0$ (i.e. variational) and higher order terms of the CBF perturbative expansion of $P(\mathbf{k}_1, \mathbf{k}_2, E)$.

3.1 The variational spectral function

At the lowest order in the perturbative expansion the spectral function is given by

$$P_{var}(\mathbf{k}_1, \mathbf{k}_2, E) = \sum_n |\langle 0 | a_{\mathbf{k}_1}^\dagger a_{\mathbf{k}_2}^\dagger | n(A-2) \rangle|^2 \delta(E - E_n^v(A-2) + E_0^v(A)) , \quad (20)$$

where the correlated states (5), and their energies $E_0^v(A)$ and $E_n^v(A-2)$ are used.

The main contributions to the sum in eq.(20) come from correlated two-hole ($2h$) and three-hole one-particle ($3h1p$) intermediate states. In the uncorrelated Fermi gas only $2h$ states contribute to $P(\mathbf{k}_1, \mathbf{k}_2, E)$, leading to the well known result

$$P_{2h,FG}(\mathbf{k}_1, \mathbf{k}_2, E) = \Theta(k_F - |\mathbf{k}_1|) \Theta(k_F - |\mathbf{k}_2|) \times \delta \left(E + \frac{\hbar^2}{2m} |\mathbf{k}_1|^2 + \frac{\hbar^2}{2m} |\mathbf{k}_2|^2 \right) , \quad (21)$$

where $\Theta(x)$ denotes the usual step function. The presence of correlations, besides changing the structure of the $2h$ contribution in the way we will discuss below, allows for nonvanishing contributions from other intermediate states, with a consequent quenching of the $2h$ peak since part of the strength is moved to higher excitation energies.

The variational $2h$ spectral function is given by:

$$P_{2h,v}(\mathbf{k}_1, \mathbf{k}_2, E) = \frac{1}{2} \sum_{\mathbf{h}_1, \mathbf{h}_2} |\Phi_{\mathbf{k}_1, \mathbf{k}_2}^{\mathbf{h}_1, \mathbf{h}_2}|^2 \Theta(k_F - |\mathbf{k}_1|) \Theta(k_F - |\mathbf{k}_2|) \times \delta(e_{h_1}^v + e_{h_2}^v + E) , \quad (22)$$

where $e_h^v = \langle \mathbf{h} | H | \mathbf{h} \rangle - E_0^v$ is the variational single particle energy and the $2h$ overlap matrix element, $\Phi_{\mathbf{k}_1, \mathbf{k}_2}^{\mathbf{h}_1, \mathbf{h}_2}$, is

$$\Phi_{\mathbf{k}_1, \mathbf{k}_2}^{\mathbf{h}_1, \mathbf{h}_2} = \langle 0 | a_{\mathbf{k}_1}^\dagger a_{\mathbf{k}_2}^\dagger | \mathbf{h}_1, \mathbf{h}_2 \rangle . \quad (23)$$

The correlated $1h$ overlap matrix element, $\Phi_{\mathbf{k}}^{\mathbf{h}} = \langle 0 | a_{\mathbf{k}}^\dagger | \mathbf{h} \rangle$, was computed in I using cluster expansion techniques. The same method is used for the $2h$ overlap, with the result that only *unlinked* cluster diagrams (*i.e.* diagrams where the points reached by the $k_{1,2}$ -lines are not connected to each other by any dynamical, $f^2 - 1$ and $f - 1$, or statistical correlations) contribute. The

linked diagrams contribution turn out to be of order $1/A$, and therefore vanish in infinite nuclear matter. Note that the factorization property of the two-nucleon momentum distribution, illustrated by eq.(11), is also a consequence of the fact that *linked* diagrams do not contribute in the $A \rightarrow \infty$ limit. The definitions, as well as the technicalities entering the cluster expansion method can be found in I and in the related references and will not be repeated here. Because of the factorization property, in nuclear matter we obtain

$$\Phi_{\mathbf{k}_1, \mathbf{k}_2}^{\mathbf{h}_1, \mathbf{h}_2} = \Phi_{\mathbf{k}_1}^{\mathbf{h}_1} \Phi_{\mathbf{k}_2}^{\mathbf{h}_2} \delta_{\mathbf{h}_1 - \mathbf{k}_1} \delta_{\mathbf{h}_2 - \mathbf{k}_2} , \quad (24)$$

the CBF expression of $\Phi_{\mathbf{k}}^{\mathbf{h}}$ being given in I (eq.(A.19)).

The correlated $2h$ spectral function retains the Fermi gas delta shaped peak. However, correlations quench the peak itself (via the $2h$ overlap matrix element) and move it to $E = -e_{h_1}^v - e_{h_2}^v$.

The $3h1p$ contribution reads

$$P_{3h1p,v}(\mathbf{k}_1, \mathbf{k}_2, E) = \frac{1}{6} \sum_{\mathbf{h}_1, \mathbf{h}_2, \mathbf{h}_3, \mathbf{p}_1} |\Phi_{\mathbf{k}_1, \mathbf{k}_2}^{\mathbf{h}_1, \mathbf{h}_2, \mathbf{h}_3, \mathbf{p}_1}|^2 \times \delta(e_{h_1}^v + e_{h_2}^v + e_{h_3}^v - e_{p_1}^v + E) , \quad (25)$$

the overlap matrix element being given by

$$\Phi_{\mathbf{k}_1, \mathbf{k}_2}^{\mathbf{h}_1, \mathbf{h}_2, \mathbf{h}_3, \mathbf{p}_1} = \langle 0 | a_{\mathbf{k}_1}^\dagger a_{\mathbf{k}_2}^\dagger | \mathbf{h}_1, \mathbf{h}_2, \mathbf{h}_3, \mathbf{p}_1 \rangle . \quad (26)$$

In the limit $A \rightarrow \infty$ the contributions of fully linked diagrams vanish in the $3h1p$ overlap as well. As a consequence,

$$\Phi_{\mathbf{k}_1 > k_F, \mathbf{k}_2 > k_F}^{\mathbf{h}_1, \mathbf{h}_2, \mathbf{h}_3, \mathbf{p}_1} = 0 . \quad (27)$$

In the other cases we obtain

$$\Phi_{\mathbf{k}_1 < k_F, \mathbf{k}_2 > k_F}^{\mathbf{h}_1, \mathbf{h}_2, \mathbf{h}_3, \mathbf{p}_1} = \sum \Phi_{\mathbf{k}_1}^{\mathbf{h}_1} \Phi_{\mathbf{k}_2}^{\mathbf{h}_2, \mathbf{h}_3, \mathbf{p}_1} \delta_{\mathbf{h}_1 - \mathbf{k}_1} , \quad (28)$$

and

$$\Phi_{\mathbf{k}_1 < k_F, \mathbf{k}_2 < k_F}^{\mathbf{h}_1, \mathbf{h}_2, \mathbf{h}_3, \mathbf{p}_1} = \sum \left[\Phi_{\mathbf{k}_1}^{\mathbf{h}_1} \Phi_{\mathbf{k}_2}^{\mathbf{h}_2, \mathbf{h}_3, \mathbf{p}_1} \delta_{\mathbf{h}_1 - \mathbf{k}_1} + \mathbf{k}_1 \leftrightarrow \mathbf{k}_2 \right] , \quad (29)$$

where the sums include all permutations of the \mathbf{h}_i indices, while the structure of the $2h1p$ overlap $\Phi_{\mathbf{k}}^{\mathbf{h}_1, \mathbf{h}_2, \mathbf{p}_1} = \langle 0 | a_{\mathbf{k}}^\dagger | \mathbf{h}_1, \mathbf{h}_2, \mathbf{p}_1 \rangle$ is discussed in I (Appendix B).

Unlike the $2h$ contribution, $P_{3h1p,v}$ is no longer delta shaped, but it is rather spread out in energy. It may be interpreted as a background contribution to be added to the two-quasiparticle part of the spectral function.

The next intermediate state to be considered is the $4h2p$ one, whose contribution may be written in terms of products of two squared $2h1p$ overlap matrix elements. However, it is numerically negligible with respect to the $3h1p$ term (several order of magnitudes smaller) and can be safely neglected.

The above intermediate states completely exhaust the momentum distribution sum rule in nuclear matter at the variational level:

$$\begin{aligned} n^v(\mathbf{k}_1, \mathbf{k}_2) &= \frac{\langle 0 | a_{\mathbf{k}_1}^\dagger a_{\mathbf{k}_2}^\dagger a_{\mathbf{k}_2} a_{\mathbf{k}_1} | 0 \rangle}{\langle 0 | 0 \rangle} = n^v(\mathbf{k}_1) n^v(\mathbf{k}_2) \\ &= \int dE P_{var}(\mathbf{k}_1, \mathbf{k}_2, E) . \end{aligned} \quad (30)$$

3.2 Perturbative corrections

The admixture of m -hole n -particle correlated states in $|\bar{N}\rangle$ originate CBF perturbative corrections. As far as the ground state is concerned, they correspond to the $n \geq 1$ terms in eq.(18).

Following the strategy developed in I, the perturbative corrections are classified as $\delta P_{GR}(\mathbf{k}_1, \mathbf{k}_2, E)$ and $\delta P_{INT}(\mathbf{k}_1, \mathbf{k}_2, E)$, coming from ground and intermediate state corrections, respectively. The total spectral function is then given by

$$P(\mathbf{k}_1, \mathbf{k}_2, E) = P_{var}(\mathbf{k}_1, \mathbf{k}_2, E) + \delta P_{GR}(\mathbf{k}_1, \mathbf{k}_2, E) + \delta P_{INT}(\mathbf{k}_1, \mathbf{k}_2, E) . \quad (31)$$

Here we consider $2h2p$ admixtures to the ground state and $2h1p$ admixtures to the $1h$ intermediate states. The first ones contribute for all $|\mathbf{k}|$ values (both below and above k_F), and their contribution can be expressed in terms of the correlation self energy $\Sigma^{CO}(\mathbf{k}, E)$, whose imaginary part is given by

$$\Im \Sigma^{CO}(\mathbf{k}, E) = \frac{\pi}{2} \sum |\langle 0 | H | \mathbf{k} \mathbf{p}_2 \mathbf{h}_1 \mathbf{h}_2 \rangle|^2 \delta(E + e_{p_2}^v - e_{h_1}^v - e_{h_2}^v) , \quad (32)$$

at $|\mathbf{k}| > k_F$ and $E < e_F^v$ and

$$\Im \Sigma^{CO}(\mathbf{k}, E) = \frac{\pi}{2} \sum |\langle 0 | H | \mathbf{p}_1 \mathbf{p}_2 \mathbf{k} \mathbf{h}_2 \rangle|^2 \delta(E + e_{h_2}^v - e_{p_1}^v - e_{p_2}^v) , \quad (33)$$

at $|\mathbf{k}| < k_F$ and $E > e_F^v$. The self energy is computed using correlated states and retaining two- and three-body separable contributions in the cluster expansion of the relevant matrix element [17].

The $2h1p$ intermediate state contribution involves the polarization self energy $\Sigma^{PO}(\mathbf{k}, E)$. The corresponding imaginary part reads

$$\Im \Sigma^{PO}(\mathbf{k}, E) = \frac{\pi}{2} \sum |\langle \mathbf{k} | H | \mathbf{p}_2 \mathbf{h}_1 \mathbf{h}_2 \rangle|^2 \delta(E + e_{p_2}^v - e_{h_1}^v - e_{h_2}^v), \quad (34)$$

at $|\mathbf{k}| < k_F$ and $E < e_F^v$ and

$$\Im \Sigma^{PO}(\mathbf{k}, E) = \frac{\pi}{2} \sum |\langle \mathbf{k} | H | \mathbf{p}_1 \mathbf{p}_2 \mathbf{h}_2 \rangle|^2 \delta(E + e_{h_2}^v - e_{p_1}^v - e_{p_2}^v), \quad (35)$$

at $|\mathbf{k}| > k_F$ and $E > e_F^v$.

The effects of these corrections on the spectral functions at $|\mathbf{k}_1|, |\mathbf{k}_2| < k_F$ are: *i*) a quenching of the variational two-quasiparticle strength and a shift of its position by a quantity $\delta e_{k_1}^{CO} + \delta e_{k_2}^{CO}(k)$, with

$$\delta e_k^{CO} = \frac{1}{\pi} \int_{e_F^v}^{\infty} dE \frac{\Im \Sigma^{CO}(\mathbf{k}, E)}{e_k^v - E}, \quad (36)$$

from ground state corrections, and *ii*) a broadening of the delta-like peak itself, roughly proportional to $\Im \Sigma^{PO}(\mathbf{k}_1, E = -e_{k_1}^v) + \Im \Sigma^{PO}(\mathbf{k}_2, E = -e_{k_2}^v)$, from intermediate state admixtures.

The expression for the total δP at $|\mathbf{k}_1|, |\mathbf{k}_2| < k_F$ reads

$$\begin{aligned} \delta P(\mathbf{k}_1, \mathbf{k}_2, E) = & -P_{2h,v}(\mathbf{k}_1, \mathbf{k}_2, E) \\ & + \frac{1}{\pi} \Im \left\{ \left[|\Phi_{\mathbf{k}_1, \mathbf{k}_2}^{\mathbf{k}_1, \mathbf{k}_2}|^2 + \Sigma_2^{PO}(\mathbf{k}_1, E) + \Sigma_2^{PO}(\mathbf{k}_2, E) \right] \right. \\ & \times \left[\alpha(\mathbf{k}_1, \mathbf{k}_2)(-e_{k_1}^v - e_{k_2}^v - E) - \delta e_{k_1} - \delta e_{k_2} \right. \\ & - \Re \left(\Sigma^{PO}(\mathbf{k}_1, E) - \Sigma^{PO}(\mathbf{k}_1, E = -e_{k_1}^v) + 1 \rightarrow 2 \right) \\ & \left. \left. - i \left(\Sigma^{PO}(\mathbf{k}_1, E) + 1 \rightarrow 2 \right) \right]^{-1} \right\}, \quad (37) \end{aligned}$$

where $\alpha(\mathbf{k}_1, \mathbf{k}_2) = 1 - \delta n_2(\mathbf{k}_1) - \delta n_2(\mathbf{k}_2) - \delta n'_2(\mathbf{k}_1) - \delta n'_2(\mathbf{k}_2)$. The quantities $\delta n_2(\mathbf{k})$, $\delta n'_2(\mathbf{k})$ and $\Sigma_2^{PO}(\mathbf{k}, E)$ are defined in I.

Fig. 3 gives two examples of the two-nucleon spectral function below k_F . The figure shows the variational one-hole ($P_{1h,v}$) and two-hole ($P_{2h,v}$) peaks and the

total spectral function (solid line). The one-nucleon spectral function below k_F can be separated into a *single particle* and a *correlated* part [18]. The former originates from $1h$ intermediate states and their admixtures, the latter from n -hole ($n - 1$)-particle states, and it would be strictly zero in absence of correlations. The corresponding contributions for the two-nucleon spectral functions are shown in the figure as dashed and dot-dash lines, respectively. The correlated part has been enhanced by a factor 10^2 , while the single particle and total ones by a factor 10. The figure also gives the barely visible variational correlated part (dotted lines).

Ground state $2h2p$ corrections give the leading contributions to δP when one of the momenta is above k_F . So, for $|\mathbf{k}_1| < k_F$ and $|\mathbf{k}_2| > k_F$, we obtain

$$\delta P(\mathbf{k}_1, \mathbf{k}_2, E) = \frac{1}{\pi} \Im \left\{ |\Phi_{\mathbf{k}_1}^{\mathbf{k}_1}|^2 \frac{\Sigma^{CO}(\mathbf{k}_2, E + e_{k_1})}{(E + e_{k_1} + e_{k_2})^2} + \Phi_{\mathbf{k}_1}^{\mathbf{k}_1} \frac{\Sigma_4^{GR}(\mathbf{k}_2, E + e_{k_1})}{E + e_{k_1} + e_{k_2}} \right\}, \quad (38)$$

where $\Sigma_4^{GR}(\mathbf{k}, E)$ is again given in I.

The spectral functions for two such cases are shown in fig. 4, together with the one-hole variational peaks corresponding to the momenta below k_F . The whole spectral function now comes from the correlated part. The figure gives the total (solid lines) and variational (dotted lines) P , as well as the perturbative corrections (dashed lines).

Corrections at $|\mathbf{k}_1|, |\mathbf{k}_2| > k_F$ are quadratic in the self energies and have not been considered.

4 Summary and conclusions

We have carried out a calculation of the nuclear matter two-nucleon spectral function $P(\mathbf{k}_1, \mathbf{k}_2, E)$ within the framework of CBF perturbation theory. The zero-th order approximation, corresponding to a variational estimate, has been supplemented with higher order corrections associated with both $2h2p$ admixture to the ground state and $2h1p$ admixtures to the $1h$ states.

The results show that the inclusion of NN interactions produces drastic changes in the behavior of $P(\mathbf{k}_1, \mathbf{k}_2, E)$, with respect to the predictions of the Fermi gas model. The peaks corresponding to the single particle states get quenched already at zero-th order, and acquire a width when higher order corrections are included. Due to strong short range NN correlations, the strength removed

from the quasi particle peak is pushed to large values of momenta and removal energy, giving rise to a broad background.

The factorization property exhibited by the two-nucleon momentum distribution of a normal Fermi liquid has been found to hold at the level of the amplitudes entering the calculation of $P(\mathbf{k}_1, \mathbf{k}_2, E)$ as well. As a result, all the linked cluster contributions to the two-nucleon spectral function vanish in the infinite nuclear matter limit.

In principle, the results discussed in this paper may be used to estimate *correlation observables*, related to the small components of $P(\mathbf{k}_1, \mathbf{k}_2, E)$, whose measurement represents the ultimate goal of the $(e, e'NN)$ experimental programs. However, it has to be emphasized that, in order to make fully quantitative predictions, our approach should be extended to finite systems, working along the line proposed in refs.[19,10]. The analysis of the A dependence of $P(\mathbf{k}_1, \mathbf{k}_2, E)$ would also provide very interesting information on the relevance of the $1/A$ linked contributions and the applicability of the factorized approximations for the two-nucleon spectral function and momentum distribution.

Acknowledgements

The authors are grateful to S. Fantoni, G.I. Lykasov, A. Polls and W.H. Dickhoff for many illuminating discussions.

References

- [1] G.E. Brown, *Many body physics*, (North-Holland, Amsterdam, 1972).
- [2] *Modern Topics in Electron Scattering*, edited by B. Frois and I. Sick (World Scientific, Singapore, 1991).
- [3] V.R. Pandharipande, I. Sick and P.K.A. deWitt Huberts, *Rev. Mod. Phys.* **69** (1997) 981.
- [4] A. Honegger *et al*, TJNAF proposal 97-006, 1997.
- [5] O. Benhar, A. Fabrocini and S. Fantoni, in *Two Nucleon Emission Reactions*, edited by O. Benhar and A. Fabrocini (ETS, Pisa, 1990)p. 49.
- [6] G. Rosner, in *Electron Nucleus Scattering*, edited by O. Benhar, A. Fabrocini and R. Schiavilla (ETS, Pisa, 1999)p. 315.
- [7] W.J.W. Geurts, K. Allaart, W.H. Dickhoff and H. Müther, *Phys. Rev. C* **54** (1996) 1144.

- [8] O. Benhar, A. Fabrocini and S. Fantoni, Nucl. Phys. **A505** (1989) 267.
- [9] S. Fantoni and V. R. Pandharipande, Nucl. Phys. **A427** (1984) 473.
- [10] G. C3, A. Fabrocini and S. Fantoni, Nucl. Phys. **A568** (1994) 73.
- [11] I. E. Lagaris and V. R. Pandharipande, Nucl. Phys. **A359** (1981) 331.
- [12] S. Fantoni, Nucl. Phys. **A363** (1981) 381.
- [13] A. Polls, private communication.
- [14] A. Ramos, A. Polls and W.H. Dickhoff, Nucl. Phys. **A503** (1989) 1.
- [15] S. Fantoni and V. R. Pandharipande, Phys. Rev. C **37** (1988) 1697.
- [16] O. Benhar, A. Fabrocini and S. Fantoni, Nucl. Phys. **A550** (1992) 201.
- [17] S. Fantoni, B. L. Friman and V. R. Pandharipande, Nucl. Phys. **A386** (1982) 1.
- [18] O. Benhar, A. Fabrocini, S. Fantoni and I. Sick, Nucl. Phys. **A579** (1994) 493.
- [19] G. C3, A. Fabrocini, S. Fantoni, and I.E. Lagaris, Nucl. Phys. **A549** (1992) 439.

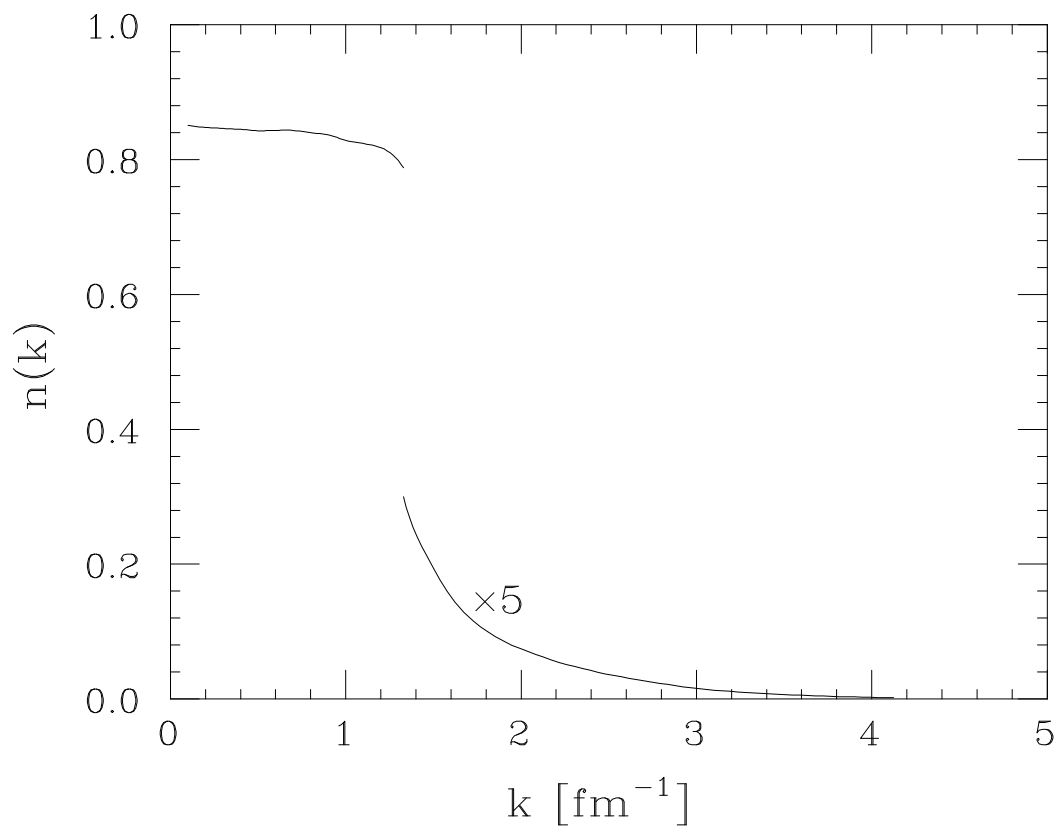


Fig. 1. Single nucleon momentum distribution in nuclear matter, evaluated in ref.[9] using CBF perturbation theory.

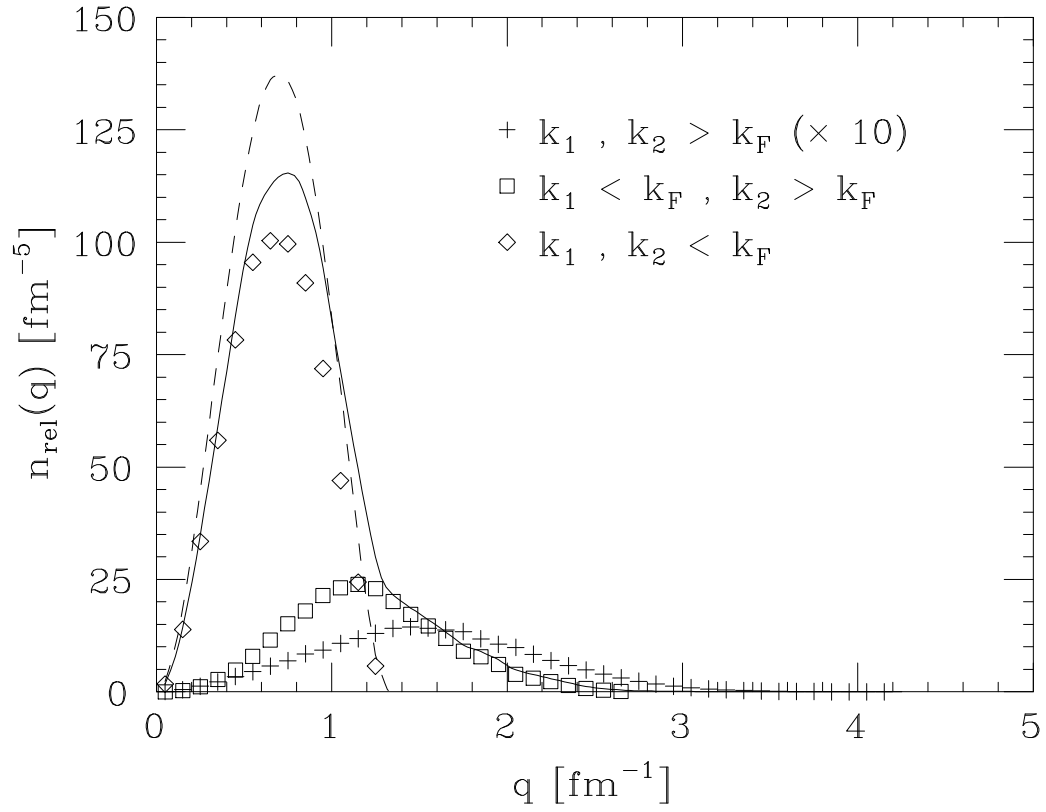


Fig. 2. The distribution $n_{rel}(\mathbf{q})$ defined in eq.(13). The solid and dashed lines represent the results obtained using CBF perturbation theory and the Fermi gas model, respectively. The meaning of the other curves is explained in the text.

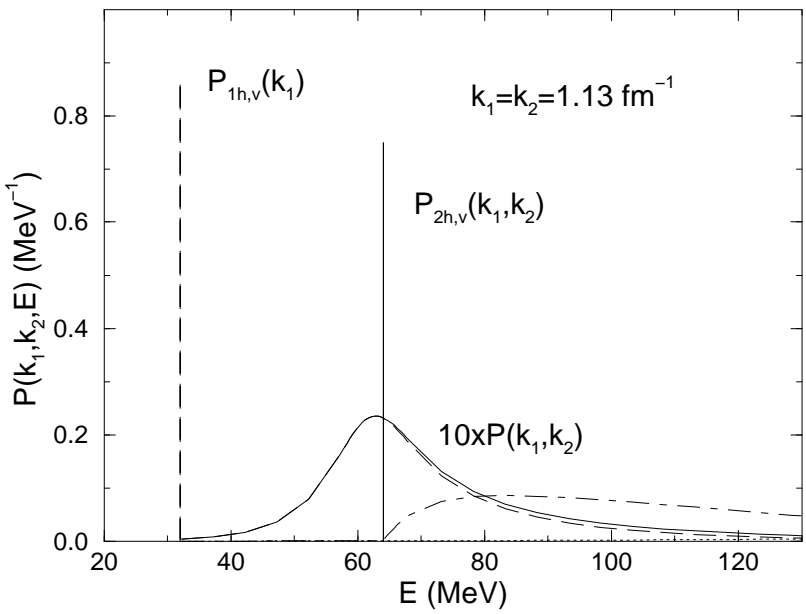
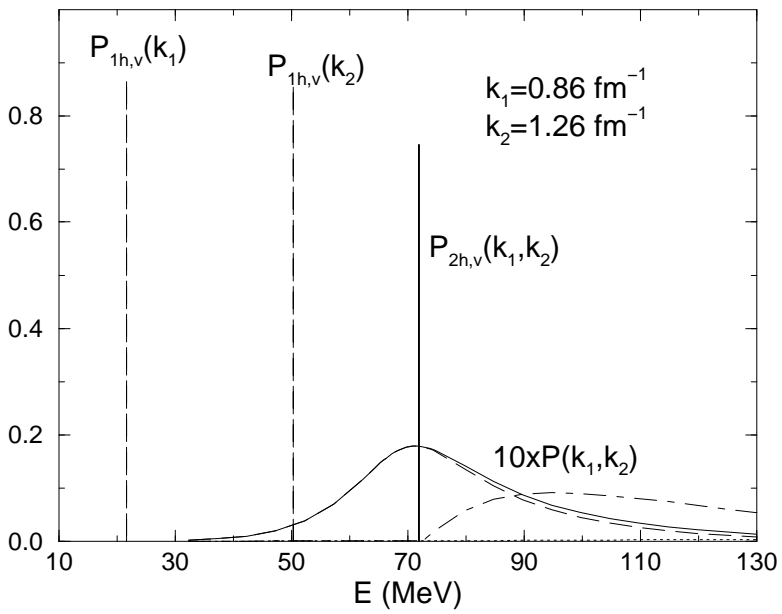


Fig. 3. Two examples of two-nucleon spectral function at $|\mathbf{k}_1|, |\mathbf{k}_2| < k_F$. The different curves are discussed in the text.

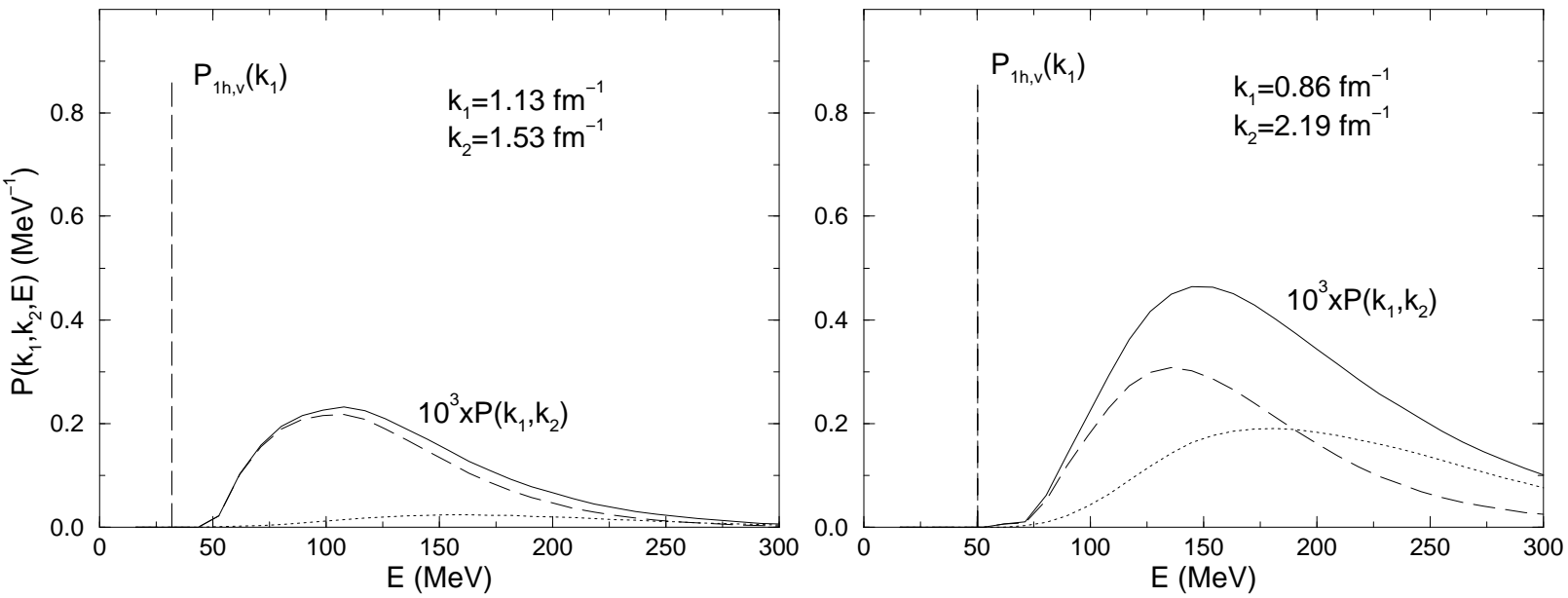


Fig. 4. Two examples of two-nucleon spectral function at $|\mathbf{k}_1| < k_F$, $|\mathbf{k}_2| > k_F$. The different curves are discussed in the text.